

# A simple rule for spike-timing-dependent plasticity: local influence of AHP current.

Anatoli Gorchetchnikov<sup>a</sup> Michael E. Hasselmo<sup>b</sup>

<sup>a</sup>*Department of Cognitive and Neural Systems, Boston University,  
677 Beacon St. Boston, MA 02215*

<sup>b</sup>*Department of Psychology, Boston University,  
64 Cummington St. Boston, MA 02215*

---

## Abstract

A classical Hebbian learning rule was adapted to produce spike-timing-dependent plasticity. The shape of the plasticity curve for this rule is shown to depend on local mechanisms such as the strength and length of afterhyperpolarization of the postsynaptic cell. The suggested rule can serve as a good approximation for network models that use simplified dynamics of membrane currents.

*Key words:* STDP, learning rule, fast AHP, quadratic integrate-and-fire

---

Recent research has focused on spike-timing-dependent plasticity (STDP) in neurons [7,8] (see [1] for review), and various implementations of the learning rules that can model this type of plasticity [3,6,9,10]. Following the general framework of [3], here we suggest a simple adaptation of a Hebbian rule that results in STDP. Similar to the rule in [3], the rule suggested here only depends on the information local to the modified synapse, i.e. it is spatially local. Unlike the rule in [3], our rule only requires the information available at this particular instance of time, i.e. it is also temporally local. Previously we demonstrated that a model of spatial navigation, which utilizes this learning rule, is capable of path learning and recall [4]. Therefore, the suggested rule was shown to work on the network level, and here we study its properties on a cellular level.

The classical Hebbian rule used in neural networks is

$$\frac{dw}{dt} = \lambda X_{pre} X_{post} \quad (1)$$

---

*Email addresses:* anatoli@cns.bu.edu (Anatoli Gorchetchnikov),  
hasselmo@bu.edu (Michael E. Hasselmo).

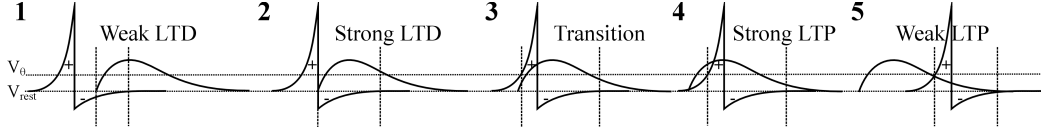


Fig. 1. Emergence of spike timing dependent plasticity (STDP) from multiplication of  $g_{syn}$  and potential at soma  $V_{soma}$ . Vertical bars show the learning window.

where  $\lambda$  is the learning rate and  $X$  are pre- and postsynaptic signals. If we assume  $X_{pre} = g_{syn}$  (synaptic conductance) and

$$X_{post} = \begin{cases} 0 & \text{if } V_{rest} < V_{soma} < V_{\theta} \\ V_{soma} & \text{otherwise} \end{cases} \quad (2)$$

then rule (1) produces STDP due to the mechanism depicted in Figure 1. A similar idea was used in [9], but they used the derivative of back-propagating action potential as  $X_{post}$ .

Note, that not only  $X_{pre}$  and  $X_{post}$  carry the information about timing of pre- and postsynaptic spikes, but also they form a learning window in a process similar to that described in [3]. Using their terminology  $X_{pre} = g_{syn}$  is the  $a$  component, while the postsynaptic potential during the spike and during fast afterhyperpolarization (fAHP) serves as  $b_+$  and  $b_-$  components, respectively.

Rule (1) can lead to unlimited weight change, and usually the limits on the weights are introduced as follows

$$\frac{dw}{dt} = \lambda X_{pre} X_{post} W_L \quad (3)$$

where  $W_L = (w - w_{MIN})(w_{MAX} - w)$ . In the simulations presented here only one of the two limiting factors is used depending on the sign of  $X_{pre}X_{post}$ . When it is positive ( $w_{MAX} - w$ ) is used, otherwise ( $w - w_{MIN}$ ) is used. These soft bounds make the weight change depend on the current weight, and, therefore, put the suggested rule in the class of multiplicative STDP rules [6].

## 1 Method

The simulated network was set up so that two principal neurons received input spikes with a certain time difference and produced their spikes in response. These two neurons were connected to each other through a plastic synapse with the parameters of the AMPA channel ( $\tau_f = \tau_r = 2ms$ ,  $E_{AMPA} = 60mV$

in equation (4) below). Transmission through recurrent connections was suppressed to prevent a possible influence on learning. Input was provided by two input neurons designed as simplified versions of a principal cell.

Principal cells use a two-compartment neuronal representation. The membrane potential in each compartment is calculated according to  $C_M \frac{dV_m}{dt} = \sum_i I_i$ , where the currents  $I_i$  include ligand gated channels and leakage in the dendritic compartment, as well as a quadratic integrate-and-fire and fast afterhyperpolarization (fAHP) current in the soma.

Ligand gated and fAHP currents were calculated as  $I_i = \frac{g_i N_i}{\pi dl} (E_i - V_m)$  where  $g_i[pS]$  is individual channel conductance and the synaptic weight  $w = \frac{N_i}{\pi dl} \left[ \frac{10^9}{cm^2} \right]$  roughly corresponds to average synaptic density in millions of channels per  $cm^2$  of the membrane. For fAHP current  $w = 1$  was assumed. Conductance was calculated according to

$$\begin{cases} g_i = \frac{\bar{g}_i p}{\tau_f - \tau_r} (e^{-\frac{t}{\tau_f}} - e^{-\frac{t}{\tau_r}}) & \text{if } \tau_f \neq \tau_r \\ g_i = \bar{g}_i \frac{t}{\tau_f} e^{(1-\frac{t}{\tau_f})} & \text{otherwise} \end{cases} \quad (4)$$

where  $\bar{g}_i[pS]$  is the maximal conductance,  $t$  is time since the presynaptic spike, and  $p$  is a scaling coefficient enforcing  $\max \left( \frac{p}{\tau_f - \tau_r} (e^{-\frac{t}{\tau_f}} - e^{-\frac{t}{\tau_r}}) \right) = 1$ .

The quadratic integrate-and-fire that was derived through Taylor expansion in [2] as  $I_i = qv_m^2 - r$ , where  $q$  scales the time course of a spike and  $r$  represents the threshold. For an in-depth discussion of dynamics and derivation of this equation see [5]. Here it is modified as

$$\begin{cases} I_i = g_i (V_m^2 - V_m V_\theta) & \text{if } V_\theta \geq V_{rest} = 0 \\ I_i = g_i \left( V_m^2 - V_m V_\theta + \frac{V_\theta^2}{2} \right) & \text{otherwise} \end{cases} \quad (5)$$

to keep the original dynamics, but to explicitly include the threshold potential  $V_\theta$  in the equation and to have the resting potential fixed at 0.

### 1.1 Simulations

In all simulations the identical set of current injections was provided to the input cells. Each run lasted 700 simulated ms, the total weight change was recorded and normalized by the number of learning episodes. Due to soft bounds on the weight that are imposed in equation (3), weight changes sum nonlinearly and such normalization could introduce a systematic error. To

prevent this, input currents were selected so that there was no systematic relationship between number of learning episodes and time difference between spikes.  $\lambda = 10^{-3}$ ,  $w_{MIN} = 0$ ,  $w_{MAX} = 5$  for all simulations. Initial value of the weight  $w \approx 1.53$  (taken from the Gaussian connectivity profile in [4]). Parameters for fAHP current were  $\tau_r = 0.1ms$  and  $E_{AHP} = -90mV$  for all simulations,  $\bar{g}_{AHP}$  and  $\tau_f$  were manipulated in two sets of simulations as follows.

*Set 1: Influence of the fAHP conductance.* Using equation (3) as a learning rule the simulations were repeated for three values of maximal fAHP conductance in equation (4):  $\bar{g}_{AHP} = 0, 0.25, 0.5$  and  $0.75pS$ . The decay time constant was fixed at  $\tau_f = 3ms$  (the effect of the fAHP current with this timing is similar to the effect of A-current in the biological neuron). We expected the increase of depression and the slight reduction of potentiation with the increase in magnitude of the AHP current.

*Set 2: Influence of fAHP timing.* Instead of varying the strength of fAHP current we varied its decay time constant. For this set  $\bar{g}_{AHP} = 0.5pS$ , and  $\tau_f = 3, 4$ , and  $5ms$ . The remaining parameters are the same. We expected that longer decay of the AHP current would result in longer lasting increase of depression. We also expected that timing of the AHP current would have smaller (if any) influence on the potentiation part of the curve.

## 2 Results

The results of two sets of simulations are presented in Figure 2. They roughly correspond to the experimental data [1] with two notable exceptions. Firstly, without the fAHP current the depression part of the curve is almost non-existent. Secondly, for all simulations the zero-crossing is shifted from 0 (or even slightly below) in [1] to  $\Delta t \approx 5ms$ . The peak of potentiation is consistently at  $\Delta t \approx 10ms$ . Not included on the plots are additional measurements at  $\Delta t \pm 60ms$  that showed no change in synaptic strengths for all conditions.

*Set 1.* The strength of the fAHP current affects both potentiation and depression. The depression part of the curve is affected much more than the potentiation part, where the influence diminishes for intervals greater than 15ms for all levels of the fAHP current. The strength of fAHP current does not affect the peak potentiation and depression timing (both stayed at  $\Delta t \approx 10ms$  and  $\Delta t \approx 0ms$ , respectively), although it does shift the peak of depression from  $\Delta t \approx 3ms$  that is observed without the fAHP.

*Set 2.* The decay time constant of the fAHP current does not affect the potentiation part of the curve much, but it has a profound effect on depression

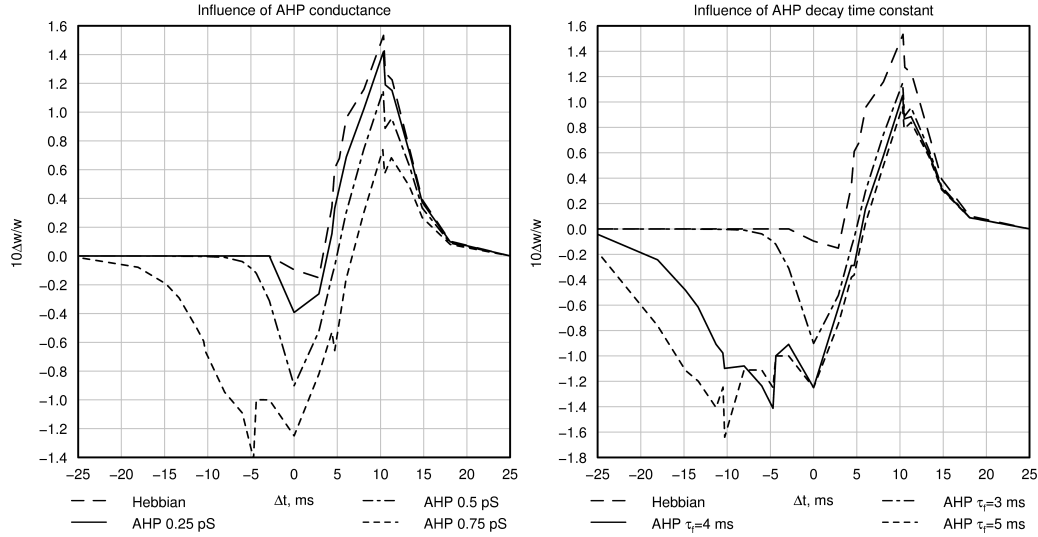


Fig. 2. STDP curves resulting from the rule (3). Left: the conductance of the AHP current varied as described in text. Right: the decay time constant of the fAHP current varied. The dash-dotted curve on both panels corresponds to parameters  $\bar{g}_{AHP} = 0.5 pS$ , and  $\tau_f = 3 ms$ . For the reference the right panel contains the long-dashed curve with no fAHP current replotted from the left panel.

part of the curve not only increasing the magnitude of depression for a longer time constant, but also shifting the peak depression backwards in time (about  $5 ms$  shift for every  $1 ms$  of  $\tau_f$  increase). This shift of the peak depression does not affect the position of the zero-crossing of the STDP curve.

### 3 Discussion

The spatially and temporally local learning rule suggested in equation (3) produces a STDP curve that qualitatively corresponds to experimental data [1] only in the presence of the fAHP current. Without the fAHP the depression part of the curve is diminished. This result follows from the shape of action potential generated by the quadratic integrate-and-fire used here (equation 5), which has very short refractory period and, therefore, effectively eliminates the  $b_-$  component from the formation of the learning window discussed in [3].

Implementation of a different spike-generating mechanism that has a longer refractory period would not require an additional fAHP, but parameters of the STDP curve would depend on parameters of refractory period the same way they were shown to depend on the fAHP current here. In addition to dependence on the shape of the action potential, rule (3) will depend on the shape of synaptic conductance, and will produce different STDP curves for different synaptic parameters. This variability of the result can account for different shapes of STDP curves observed experimentally in different cell types.

The positive shift in zero-crossing observed here can be eliminated by using the delayed in time back-propagating action potential instead of the real spike used here. This approach would make the resulting rule closer to the rule suggested in [9], but it would require an increase in the complexity of the model. Overall, the suggested rule showed reasonable performance and can be used in the models where simplicity and computational cost have priority over biological details. More research is necessary to determine how close it can approximate the experimental data collected in various conditions.

## References

- [1] G.-q. Bi and M.-m. Poo, Synaptic modification by correlated activity: Hebb's postulate revisited, *Annu Rev Neurosci*, 24 (2001) 139–166.
- [2] G. B. Ermentrout and N. Kopell, Parabolic bursting in an excitable system coupled with slow oscillation, *SIAM J Appl Math*, 46 (1986) 233–252.
- [3] W. Gerstner, R. Kempter, J. L. van Hemmen, and H. Wagner, Hebbian learning of pulse timing in the Barn Owl auditory system, in: W. Maass and C. M. Bishop, eds., *Pulsed Neural Networks*, (MIT Press, Cambridge, MA, 1999) chapter 14, 353–377.
- [4] A. Gorchetchnikov and M. E. Hasselmo, Rhythmic neuromodulation and spike timing dependent plasticity in the model of rat spatial navigation, *Soc Neurosci Abstr*, 33 (2003) 91.17.
- [5] F. C. Hoppensteadt and E. M. Izhikevich, *Weakly Connected Neural Networks*, (Springer-Verlag, New York, NY, 1998).
- [6] A. Kepeks, M. C. V. van Rossum, S. Song, and J. Tegner, Spike-timing-dependent plasticity: Common themes and divergent vistas, *Biol Cybern*, 87 (2002) 446–458.
- [7] W. B. Levy and O. Steward, Temporal contiguity requirements for long-term associative potentiation/depression in the hippocampus, *Neuroscience*, 8, 4 (1983) 791–797.
- [8] H. Markram, J. Lubke, M. Frotscher, and B. Sakmann, Regulation of synaptic efficacy by coincidence of postsynaptic APs and EPSPs, *Science*, 275 (1997) 213–215.
- [9] B. Porr, A. Saudargiene, and F. Wörgötter, Analytical solution of spike-timing dependent plasticity based on synaptic biophysics, in: S. Thrun, L. Saul, and B. Schölkopf, eds., *Advances in Neural Information Processing Systems 16*, (MIT Press, Cambridge, MA, 2004).
- [10] S. Song, K. D. Miller, and L. F. Abbott, Competitive Hebbian learning through spike-timing-dependent synaptic plasticity, *Nature Neurosci*, 3 (2000) 919–926.